Reducing spectral attenuation in small-core photonic crystal fibers

I. Gris-Sánchez,* B.J. Mangan, and J.C. Knight

Centre for Photonics and Photonic Materials, Department of Physics, University of Bath, Claverton Down, Bath BA2 7AY, United Kingdom

**I.Gris.Sanchez@bath.ac.uk*

Abstract: We describe a modified fabrication process to reduce spectral attenuation in highly nonlinear photonic crystal fibers (PCF) by reducing the effect of OH^- content in the silica glass. In particular we show outstanding results for small core sizes of 2μm diameter including an attenuation of 10dB/km at the OH^- peak wavelength of 1384nm, by annealing the preform prior to the fiber draw.

OCIS codes: (060.4005) Microstructured fibers; (060.0060) Fiber Optics and Optical Communications.

References and links

1. A. Kudlinski, G. Bouwmans, O. Vanvincq, Y. Quiquempois, A. Le Rouge, L. Bigot, G. Mélin, and A. Mussot, "White-light cw-pumped supercontinuum generation in highly GeO(2)-doped-core photonic crystal fibers," Opt. Lett. **34**(23), 3631–3633 (2009).
2. B. A. Cumberland, J. C. Travers, S. V. Popov, and J. R. Taylor, "Toward visible cw-pumped supercontinua," Opt. Lett. **33**(18), 2122–2124 (2008).
3. J. C. Travers, R. E. Kennedy, S. V. Popov, J. R. Taylor, H. Sabert, and B. Mangan, "Extended continuous-wave supercontinuum generation in a low-water-loss holey fiber," Opt. Lett. **30**(15), 1938–1940 (2005).
4. C. Guo, S. Ruan, P. Yan, E. Pan, and H. Wei, "Flat supercontinuum generation in cascaded fibers pumped by a continuous wave laser," Opt. Express **18**(11), 11046–11051 (2010).
5. W. Wadsworth, N. Joly, J. Knight, T. Birks, F. Biancalana, and P. Russell, "Supercontinuum and four-wave mixing with Q-switched pulses in endlessly single-mode photonic crystal fibres," Opt. Express **12**(2), 299–309 (2004).
6. J. M. Stone and J. C. Knight, "Visibly "white" light generation in uniform photonic crystal fiber using a microchip laser," Opt. Express **16**(4), 2670–2675 (2008).
7. S. A. Dekker, R. Pant, A. C. Judge, C. Martijn de Sterke, B. J. Eggleton, I. Gris-Sánchez, and J. C. Knight, "Highly-Efficient, Octave Spanning Soliton Self Frequency Shift Using a Photonic Crystal Fiber with Low OH Loss," in Frontiers in Optics, OSA Technical Digest (CD)(Optical Society of America, 2010), PDPB6. *http://www.opticsinfobase.org/abstract.cfm?URI=FiO-2010-PDPB6*
8. J. D. Harvey, R. Leonhardt, S. Coen, G. K. L. Wong, J. C. Knight, W. J. Wadsworth, and P. St.J. Russell, "Scalar modulation instability in the normal dispersion regime by use of a photonic crystal fiber," Opt. Lett. **28**(22), 2225–2227 (2003).
9. O. Humbach, H. Fabian, U. Grzesik, U. Haken, and W. Heitmann, "Analysis of OH absorption bands in synthetic silica," J. Non-Cryst. Solids **203**, 19–26 (1996).
10. J. Stone and G. E. Walrafen, "Overtone vibrations of OH groups in fused silica optical fibers," J. Chem. Phys. **76**(4), 1712–1722 (1982).
11. M. Nielsen, C. Jacobsen, N. Mortensen, J. Folkenberg, and H. Simonsen, "Low-loss photonic crystal fibers for transmission systems and their dispersion properties," Opt. Express **12**(7), 1372–1376 (2004).
12. M. Nielsen, N. Mortensen, M. Albertsen, J. Folkenberg, A. Bjarklev, and D. Bonacinni, "Predicting macrobending loss for large-mode area photonic crystal fibers," Opt. Express **12**(8), 1775–1779 (2004).
13. K. Tajima, "Low loss PCF by reduction of hole surface imperfection," Eur. Conf. Optical Commun. (ECOC) (2007) Paper PD2.1.
14. R. T. Bise and D. J. Trevor, "Surface absorption in microstructured optical fibers," in Optical Fiber Communication Conference, Technical Digest (CD) (Optical Society of America, 2004), paper WI4, *http://www.opticsinfobase.org/abstract.cfm?URI=OFC-2004-WI4*
15. K. Kurokawa, K. Nakajima, K. Tsujikawa, T. Yamamoto, and K. Tajima, "Ultra-wideband transmission over low loss pcf," J. Lightwave Technol. **27**(11), 1653–1662 (2009).
16. M.-C. Phan-Huy, J.-M. Moison, J. A. Levenson, S. Richard, G. Mélin, M. Douay, and Y. Quiquempois, "Surface Roughness and Light Scattering in a Small Effective Area Microstructured Fiber," J. Lightwave Technol. **27**(11), 1597–1604 (2009).
17. P. Roberts, F. Couny, H. Sabert, B. Mangan, T. Birks, J. Knight, and P. Russell, "Loss in solid-core photonic crystal fibers due to interface roughness scattering," Opt. Express **13**(20), 7779–7793 (2005).

#143230 - $15.00 USD Received 24 Feb 2011; revised 11 Apr 2011; accepted 21 Apr 2011; published 2 May 2011

18. P. Kaiser, "Drawing-induced coloration in vitreous silica fibers," J. Opt. Soc. Am. **64**(4), 475–481 (1974).
19. Y. Hayashi, Y. Okuda, H. Mitera, and K. Kato, "Formation of Drawing or Radiation-Induced Defects in Germanium Doped Silica Core Optical Fiber," Jpn. J. Appl. Phys. **33**(Part 2, No. 2B), L233–L234 (1994).
20. J. C. Knight, T. A. Birks, P. St. J. Russell, and D. M. Atkin, "All-silica single-mode optical fiber with photonic crystal cladding," Opt. Lett. **21**(19), 1547–1549 (1996).
21. A. Monteville, D. Landais, O. Le Goffic, D. Tregoat, N. J. Traynor, T. Nguyen, S. Lobo, T. Chartier, and J. Simon, "Low Loss, Low OH, Highly Non-linear Holey Fiber for Raman Amplification," in Conference on Lasers and Electro-Optics/Quantum Electronics and Laser Science Conference and Photonic Applications Systems Technologies, Technical Digest (CD) (Optical Society of America, 2006), paper CMC1, *http://www.opticsinfobase.org/abstract.cfm?URI=CLEO-2006-CMC1*
22. K. Tajima, J. Zhou, K. Nakajima, and K. Sato, "Ultralow Loss and Long Length Photonic Crystal Fiber," J. Lightwave Technol. **22**(1), 7–10 (2004).
23. K. Tajima, J. Zhou, K. Kurokawa, and K. Nakajima, "Low water peak photonic crystal fibers," 29th European conference on optical communication ECOC'03 (Rimini, Italy), pp. 42–43 (2003).
24. I. Gris-Sánchez, B. J. Mangan, and J. C. Knight, "Reducing Spectral Attenuation in Solid-Core Photonic Crystal Fibers," in Optical Fiber Communication Conference, OSA Technical Digest (CD) (Optical Society of America, 2010), paper OWK1. *http://www.opticsinfobase.org/abstract.cfm?URI=OFC-2010-OWK1*
25. Heraeus, "High purity rods". *http://heraeus-quarzglas.com/media/webmedia_local/downloads/broschren_sf/2009_sf/PCF.pdf*
26. Heraeus, "Quartz glass for optics data and properties" *http://www.heraeus-quarzglas.com/media/webmedia_local/downloads/broschren_mo/SO_Data_and_properties_* EN.pdf.
27. L. Nuccio, S. Agnello, and R. Boscaino, "Intrinsic generation of OH groups in dry silicon dioxide upon thermal treatments," Appl. Phys. Lett. **93**(15), 151906 (2008).
28. L. Nuccio, S. Agnello, and R. Boscaino, "Annealing of radiation induced oxygen deficient point defects in amorphous silicon dioxide: evidence for a distribution of the reaction activation energies," J. Phys. Condens. Matter **20**(38), 385215 (2008).
29. R. K. Iler, *The Chemistry of Silica* (John Wiley and Sons, New York, 1979), Chap 6.
30. R. H. Doremus, *Glass Science*, (John Wiley and Sons, New York, 1973), Chap 7.
31. E. J. Friebele, G. H. Sigel, and D. L. Griscom, "Drawing-induced defect centers in a fused silica core fiber," Appl. Phys. Lett. **28**(9), 516–518 (1976).
32. Y. Hibino and H. Hanafusa, "Defect structure and formation mechanisms of drawing-induced absorption at 630nm in silica optical fibers," J. Appl. Phys. **60**(5), 1797–1801 (1986).
33. H. Mehrer, *Diffusion in Solids* (Springer-Verlag Berlin Heidelberg, 2007), Chap 6.

1. Introduction

In solid core photonic crystal fibers (PCF) with small core sizes, achieving the lowest possible spectral attenuation is important for applications like supercontinuum generation [1–6], soliton self-frequency shift [7] and parametric conversion processes [8]. Absorption lines of OH^- ions in silica, particularly at 1384nm [9,10], limit the applications of PCF, reducing the intensity of transmitted light at certain wavelengths. The attenuation at 1384nm due to OH^- increases dramatically when the core size is decreased. Review of the available literature [11,12] shows that attenuation at this wavelength increases by orders of magnitude, typically above 30dB/km and up to several hundreds of dB/km for core diameters in the range below 2μm. The attenuation at other wavelengths not corresponding to known OH^- absorption bands also increases because of increased surface scattering [13–17] and because of the creation of defect sites within the silica lattice arising from the fabrication process (e.g. the drawing induced band around 630nm wavelength) [18,19].

The aim of our work was to reduce the attenuation in solid-core PCF fabricated using the stack-and-draw process [20], in particular for cores sizes below 2μm. In this regime the attenuation is dominated by surface scattering and OH^- content [21–23]. In [24] we demonstrated that changes in the preform in the hours after it had been drawn from the stack strongly affected the final fiber attenuation, and we presented two different methods to reduce the attenuation due to the presence of OH^- ions. These methods were intended to address the extrinsic OH^- attenuation due to adsorption of atmospheric hydroxyl onto the silica surfaces during preform preparation and subsequent diffusion into the fiber core during drawing. In that previous work, rapid processing was shown to avoid increased attenuation [24] as illustrated in Fig. 1, where the lowest attenuation is obtained with the quickest turnaround time. Neither approach described in the previous work is especially suitable or easy to implement for complex preforms, where longer timescales and increased exposure of the drawn materials to the atmospheric moisture is more likely. We now propose an alternative

#143230 - $15.00 USD Received 24 Feb 2011; revised 11 Apr 2011; accepted 21 Apr 2011; published 2 May 2011

approach that reduces the effects of extrinsic OH^- in contaminated canes. The attenuation level obtained with our modified fabrication process for an all-silica 2μm core PCF is the lowest reported for such a small core [21] using commercially available synthetic silica glass [25,26]. The OH^- concentration observed in the final fiber is close to that specified for the starting material. However, in [27] it was shown that the OH^- content of dry synthetic silica may change with thermal treatment, and we cannot preclude this in our experiments.

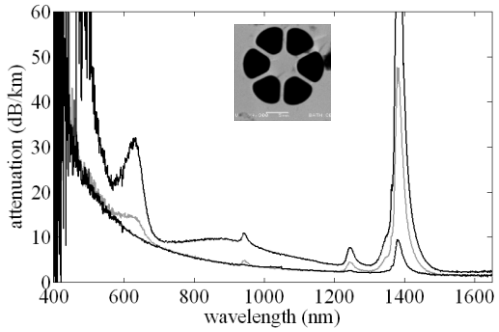

Fig. 1. Spectral attenuation for three different fibers drawn after different delays. Bottom to top: 3 hours, 18 hours (gray line) and 7 days. With longer delays, attenuation increases at short wavelengths (<600nm), 630nm, 1384nm, and a broadband peak at 900nm appears [18]. Inset: SEM of a 5μm core fiber as used in experiments.

The spectra shown in Fig. 1 were obtained from PCF's fabricated using the standard stack and draw process [20] and Suprasil F300 as the starting material. Although the exact concentration of OH^- in the starting material is not known, the manufacturer's specification is below 1ppm and is quoted to be typically 0.2ppm. This corresponds to an attenuation of 12.1dB/km at 1384nm [9]. The fibers fabricated have different levels of attenuation at this wavelength, ranging from 8dB/km for large core diameters (e.g. 5μm and above) to as much as 200dB/km for untreated small-core fibers suggesting that additional OH^- becomes significantly more of a problem for small core fibers.

The additional processing step introduced in this paper consists of annealing [28–30] the preform at high temperature in a nitrogen atmosphere immediately prior to drawing the fiber. This has the effect of relaxing the silica network, passivating defect sites while simultaneously removing the OH^- that may have adsorbed onto the surfaces during the fabrication process. Such OH^- may diffuse into the core of the fiber and/or lead to surface distortion by the $SiOH^-$ groups just below the surface [29]. The effect of the annealing process on the attenuation of the fiber is to reduce the level of OH^- (most evident at 1384nm) in the fiber core whilst the attenuation peak at 630nm [18] (Fig. 2a) that is related to the stresses in the silica matrix [24,31,32] is effectively eliminated. We speculate that by healing lattice defects, the annealing removes bonding sites and thus reduces the diffusion of OH^- ions through the silica matrix by the vacancy mechanism [33].

2. Fabrication process

For the new results to be presented in this paper, the fiber structure consists of a solid pure silica core surrounded by three rings of air holes as shown in Fig. 2a inset. The raw material used for the core rod was Suprasil F500 synthetic silica from Heraeus while the material used for capillaries was Suprasil F300. The two materials are nominally identical except that the F500 has a significantly lower OH^- content, typically 0.02ppm compared to 0.2ppm for F300. Note that the actual fiber core includes material from both the core rod and also the surrounding capillaries. For the results presented here the total time to fabricate the stack was approximately 7 hours. The stack remained in the clean room until the next day when it was drawn down to 2mm diameter canes which were then stored in a N_2 atmosphere. The room temperature and the relative humidity while fabricating the stack were 20°C and 30% respectively.

#143230 - $15.00 USD Received 24 Feb 2011; revised 11 Apr 2011; accepted 21 Apr 2011; published 2 May 2011

Each cane was placed inside a thick-walled F300 jacketing tube in order to ensure an acceptably large outer diameter of the final fiber. The jacketed cane (which formed the preform for the fiber draw) was continuously purged with nitrogen from one end whilst being passed through the fiber-drawing furnace at 20mm/min. The furnace temperature was set so that the pyrometer reading was at 1880°C. This process was repeated three times before the fiber was drawn in the usual way. The fibers were characterized within 7 days of their fabrication. The annealing conditions were chosen because they gave good results. Higher annealing temperatures and longer annealing times led to unacceptable distortion of the fiber structure, whilst shorter times were less effective at reducing attenuation.

3. Experiments

In Fig. 2a we show the spectral attenuation for two fibers drawn from two identical canes from the same stack, with core diameters of 2μm. The fiber with lower attenuation was obtained by using the additional annealing step whereas the fiber fabricated with no special treatment giving higher attenuation is used as a reference to compare the effectiveness of the annealing process. The unprocessed fiber attenuation is characterized by a large OH^- peak at 1384nm, smaller OH^- peaks at 950 and 1250 nm, and the appearance of a significant drawing-induced absorption band at 630nm (34dB/km). The processed fiber has virtually no 630nm peak, an OH^- attenuation of 10dB/km at 1384nm, and reduced background attenuation. This level of OH^- absorption is associated with an OH^- concentration of 0.16ppm. The background attenuation is assumed to be related to light scattered due to surface roughness [16,17]. Roughness can have different origins, with one of them being OH^- contamination [30]. We attribute the disappearance of the 630nm peak to the thermal healing of lattice defects as described earlier. This attenuation at 1384nm is the lowest OH^- concentration value reported for a 2μm core fiber. Through the study of multiple fibers we observe that the appearance of the drawing-induced band at 630nm (resulting from lattice defects) is commonly accompanied by an increased attenuation at 1384nm due to OH^- absorption.

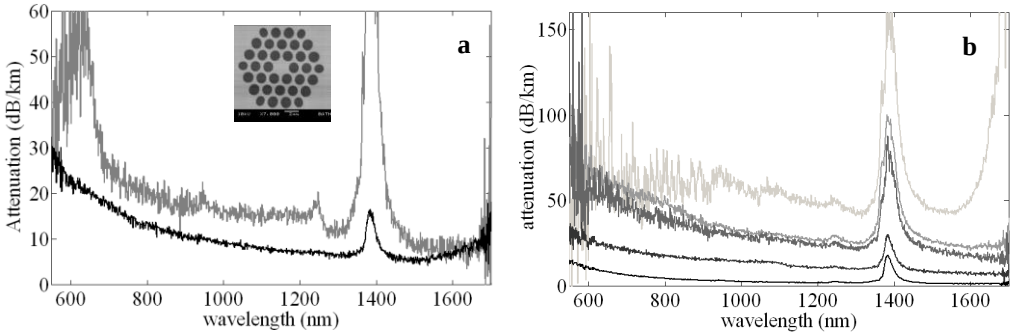

Fig. 2. a) Spectral attenuation of two fibers with a core of 2μm. Black curve: spectral attenuation of a solid core PCF obtained after the annealing process. Gray curve: spectral attenuation obtained from an identical fiber without the treatment. Inset: SEM of a 2μm core fiber as used in experiments. b) Comparison of the spectral attenuation for solid core PCF with different core sizes using an annealed preform. From top to bottom: 1.2, 1.4, 1.5, 2 and 6μm core diameter.

Subsequently, using a different annealed preform, a new set of fibers was fabricated to investigate the dependence of the attenuation on the fiber core diameter. Figure 2b shows the attenuation obtained from fibers of different core diameters (2.0, 1.5, 1.4 and 1.2μm) drawn, in that order, from the same cane during the same draw (draw speed and temperature settings were changed when reducing the fiber diameter). The tension (190g) and draw speed (32m/min) to obtain fibers with core diameters from 2μm and above were kept very similar. For fibers with core sizes below 2μm, the tension was lower (140g) to avoid fiber break, and the draw speed was slightly higher (up to 42m/min).

#143230 - $15.00 USD Received 24 Feb 2011; revised 11 Apr 2011; accepted 21 Apr 2011; published 2 May 2011

This Fig. 2b also includes the attenuation results obtained for a 6.0μm core fiber from an identical experiment to illustrate the difference in attenuation for larger core size. The low attenuation results are repeatable using different canes. We also have observed spectral features at short wavelengths (below 600nm) previously attributed to macrobending losses [12], at 900nm (a broadband peak) [18,24] and long wavelengths (above 1600nm) perhaps related to defects or OH^- levels. These effects are worthy of further study but are simply noted here.

4. Discussion

The magnitude of the attenuation observed at 1384nm measured for a different set of fibers, as a function of the core diameter, is shown in Fig. 3. The OH^- absorption is almost constant at approximately 20dB/km for core diameters above 2 μm but then increases very rapidly to over 100dB/km for 1.2μm core diameter. An increase in the background scattering loss is also observed.

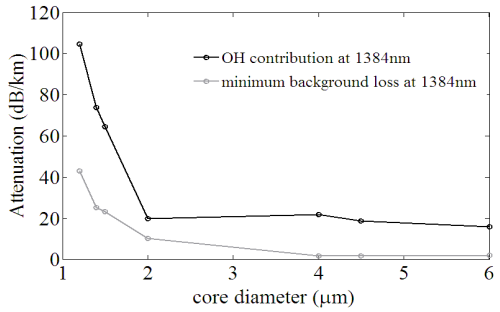

Fig. 3. The measured attenuation at the OH^- peak wavelength of 1384nm increases dramatically for core sizes below 2um. The background loss component due to scattering also increase for small core sizes.

We have considered various explanations for the observed strong dependence of attenuation on core diameter. It is known that the losses due to surface scattering increase strongly for smaller core sizes [16] but the wavelength dependence of such losses precludes this being directly responsible for the observed attenuation peaks. The "draw band" at 630nm is usually associated with damage to the silica network during the drawing process [18], and might be expected to increase if the same size preform is drawn to a smaller final fiber, as in our experiments. The presence of a greater density of lattice defects might then facilitate the diffusion of hydrogen atoms or OH^- ions into the core by vacancy hopping [33]. A third possibility is that contaminants (hydrogen or OH^-) introduced onto the silica surfaces diffuse only a short absolute distance into the core during subsequent fiber drawing. For large cores, this would result in contamination of only a small fraction of the total core area and therefore only a limited overlap with the guided mode profile. For smaller cores the same absolute distance of OH^- ingress would make up much more of the core size and result in an increase of the overlap of the guided mode with the OH^- contaminated glass.

In order to investigate this third possibility we have performed numerical simulations using the finite element method (FEM) to calculate the power of the fundamental mode as a function of distance from the core surface. The simulations were performed for a strand of silica surrounded by air which is a good approximation to the highly nonlinear PCF used in our experiments. The core is defined here as a pure uncontaminated silica rod surrounded by a ring of OH^- doped silica of thickness given by the suggested diffusion length of OH^- into silica. We calculated the ratio between the power of the fundamental mode that overlaps with the contaminated ring (P_{ring}) and the total power of the mode (P_{total}), $P_{ratio} = P_{ring}/P_{total}$, and plotted it for different conjectured diffusion lengths for different core sizes as shown in Fig. 4. The simulations were performed for diffusion lengths from 0.10μm to 0.80μm and for core diameters from 1μm to 6μm.

#143230 - $15.00 USD Received 24 Feb 2011; revised 11 Apr 2011; accepted 21 Apr 2011; published 2 May 2011

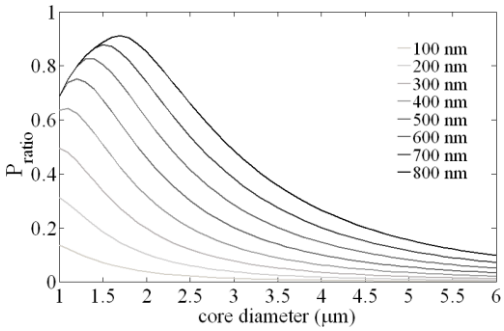

Fig. 4. The ratio (represented by P_{ratio}) between the power of the fundamental mode contained within a diffusion ring starting at the core surface and the total power. Each line is calculated for diffusion lengths ranging from 0.1μm to 0.8μm and plotted for core diameters from 1μm to 6μm. Curves do not go to unity because some of the total power resides outside the core.

It is observed that although most of the simulated curves (Fig. 4) increase significantly for core diameters below 2μm, even the most rapid increase of these calculated curves is not nearly enough to explain the experimental observation shown in Fig. 3. When combined with the observation of a correlation between the appearance of the 630nm band and increased OH^- absorption we conclude that this suggests that the appearance of a greatly increased number of lattice defect sites in the smaller-core fibers (as a result of their being drawn to a greater extent, and more rapidly) is a possible explanation for the stronger dependence of spectral attenuation on core diameter than anticipated in Fig. 4.

The OH^- concentration is related to the height of the 1384nm peak which increases significantly for smaller core sizes. As the attenuation for these small core fibers is much higher than that specified in the raw material it appears likely that the extra OH^- contamination is due to extrinsic OH^- diffusing from the surfaces of the silica into the bulk medium. The extrinsic OH^- diffuses through silica by diverse mechanisms [33]. There may be a contribution from intrinsic OH^- formation as well [27], but we have not investigated that.

5. Conclusions

We have demonstrated an annealing process that reduces attenuation in small-core photonic crystal fibers to the lowest levels reported. The effect of the annealing is to reduce spectral absorption associated with OH^- while eliminating the drawing-induced absorption band at 630nm wavelength and also reducing the overall background attenuation generally attributed to scattering. There remains a strong residual dependence of the OH^- absorption features and the background scattering losses on core diameter for core diameters below 2μm. Using numerical simulations we have shown that this strong dependence cannot be explained by the diffusion depth of OH^- ions from the surfaces alone. Instead, we tentatively attribute it to the rapid increase in the number and density of drawing-induced defect sites in the silica lattice when the preform is drawn to smaller diameters. To understand the contribution of each OH^- source in the final fiber (extrinsic or intrinsic) a deeper study of the material would be necessary.

Acknowledgments

We would like to acknowledge Dr. James Stone for useful discussions. This work has been part funded by the EU FP7 programme "CARS EXPLORER" and the UK Engineering and Physical Sciences Research Council. IGS acknowledges the Mexican Council for Science and Technology (CONACyT) for financial support.

#143230 - $15.00 USD Received 24 Feb 2011; revised 11 Apr 2011; accepted 21 Apr 2011; published 2 May 2011